

Integrated Micromechanical Circuits for RF Front Ends

Clark T.-C. Nguyen
 Dept. of Electrical Engineering and Computer Science
 University of Michigan
 Ann Arbor, Michigan 48105-2122 USA
 E-mail: ctnguyen@umich.edu

Abstract—Having now produced devices with sufficient Q , thermal stability, aging stability, and manufacturability, vibrating RF MEMS technology is already finding its way into next generation timing and wireless applications. At this juncture, the technology is now poised to take its next logical steps: higher levels of circuit complexity and integration. In particular, as vibrating RF MEMS devices are perceived more as circuit building blocks than as stand-alone devices, and as the frequency processing circuits they enable become larger and more complex, the makings of an integrated micromechanical circuit technology begin to take shape, perhaps with a functional breadth to rival that of integrated transistor circuits. After briefly reviewing the present state of vibrating RF MEMS device technology, this paper suggests the mechanical circuit element attributes most likely to insure a broad functional range for future integrated micromechanical circuits.

Keywords—MEMS, micromechanical, quality factor, resonator, oscillator, filter, wireless communications, mechanical circuit, LSI, VLSI, RF MEMS.

I. INTRODUCTION

Today's wireless transceivers are designed under a near mandate to minimize or eliminate, in as much as possible, the use of high- Q passives. The reasons for this are quite simple: cost and size. Specifically, the ceramic filters, SAW filters, quartz crystals, and now FBAR filters, capable of achieving the Q 's from 500-10,000 needed for RF and IF bandpass filtering and frequency generation functions, are all off-chip components that must interface with transistor functions at the board-level, taking up a lot of board space, and comprising a sizable fraction of the parts and assembly cost.

Pursuant to reducing the off-chip parts count in modern cellular handsets, direct-conversion receiver architectures [1] have removed the IF filter, and integrated inductor technologies are removing some of the off-chip L 's used for bias and matching networks [2]. Although these methods can lower cost, they often do so at the expense of increased transistor circuit complexity and more stringent requirements on circuit performance (e.g., dynamic range), both of

which degrade somewhat the robustness and power efficiency of the overall system. In addition, the removal of the IF filter does little to appease the impending needs of future multi-band reconfigurable handsets that will likely require high- Q RF filters in even larger quantities—perhaps one set for each wireless standard to be addressed. Fig. 1 presents the simplified system block diagram for a handset receiver targeted for multi-mode applications, clearly showing that it is the high- Q RF filters, not the IF filter, that must be addressed. In the face of this need, and without a path by which the RF filters can be removed, an option to reinsert high Q components without the size and cost penalties of the past would be most welcome, especially if done in a manner that allows co-integration of passives with transistors onto the same chip.

Recent advances in vibrating RF MEMS technology [3]-[5] have yielded micromechanical resonators with Q 's greater than 10,000 at GHz frequencies [6]-[8], thermal stabilities down to 18 ppm over 27-107°C [9], impressive aging characteristics [10]-[11], and antenna-matchable impedances [12]. Indeed, with some of the above attributes superior to those attainable by macroscopic counterparts, the technical argument for the use of vibrating RF MEMS as high- Q replacement components in existing wireless subsystems is already quite strong. As a result, vibrating micromechanical devices are presently strong candidates for

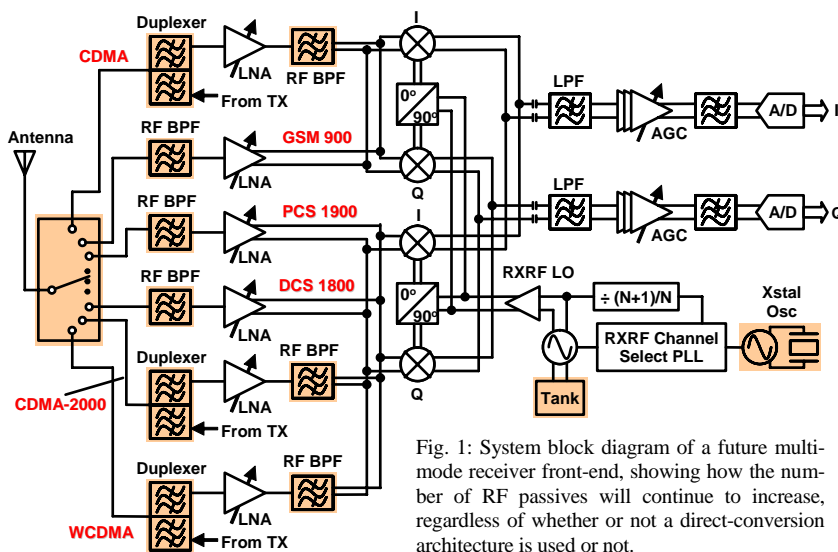


Fig. 1: System block diagram of a future multi-mode receiver front-end, showing how the number of RF passives will continue to increase, regardless of whether or not a direct-conversion architecture is used or not.

inclusion into a number of future wireless communication sub-systems, from cellular handsets, to PDA's, to low-power networked sensors, to ultra-sensitive radar and jam-resistant communicators designed for hostile environments. Indeed, piezoelectric thin-film bulk acoustic resonators (FBAR's) [13][14], composed of deposited piezoelectric materials sandwiched between metal electrodes that drive them into extensional-mode vibration, have already become a successful high volume MEMS product in the wireless handset arena. And at the time of this writing, timekeeper products based on vibrating MEMS technology stand poised to impact the voluminous frequency control market.

But the benefits afforded by vibrating RF MEMS technology go far beyond mere component replacement. In fact, the extent to which they offer performance and economic benefits grows exponentially as researchers and designers begin to perceive these devices more as on-chip building blocks than as discrete stand-alone devices. In particular, by mechanically linking vibrating mechanical structures into more general networks, "integrated micromechanical circuits" can be conceived capable of implementing virtually any signal processing function presently realizable via transistor circuits, and with potential power and linearity advantages, especially for functions that involve frequency processing. In essence, micromechanical linkages might form the basis for an integrated micromechanical circuit technology with a breadth of functionality to rival that of transistor integrated circuits. Among the application possibilities are reconfigurable RF channel-selecting filter banks, ultra-stable reconfigurable oscillators, frequency domain computers, and frequency translators. When further integrated together with other micro-scale devices (e.g., transistors, micro-ovens, micro-coolers, atomic cells), system-level benefits for portable applications abound, particularly those for which architectural changes allow a designer to trade high Q for lower power consumption and greater robustness, with potentially revolutionary impact.

After briefly describing and reviewing the present state of vibrating RF MEMS device technology, this paper considers circuits of such devices and attempts to suggest the MEMS technologies and attributes most suitable to enabling a generalized integrated micromechanical circuit platform.

II. MEMS TECHNOLOGY

There are now a wide array of MEMS technologies capable of attaining on-chip micro-scale mechanical structures, each distinguishable by not only the type of starting or structural material used (e.g., silicon, silicon carbide, glass, plastic, etc.), but also by the method of micromachining (e.g., surface, bulk, 3D growth, etc.), and by the application space (e.g., optical MEMS, bio MEMS, etc.). For the present focus on timing and portable communications, MEMS technologies amenable to low capacitance merging of micromechanical structures together with integrated transistor circuits are of high interest.

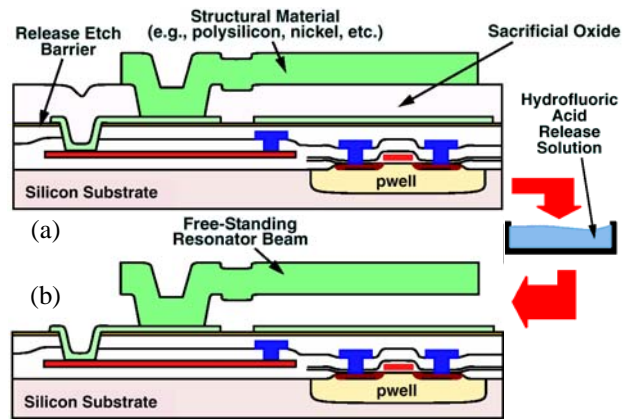


Fig. 2: Cross-sections (a) immediately before and (b) after release of a surface-micromachining process done directly over CMOS [15].

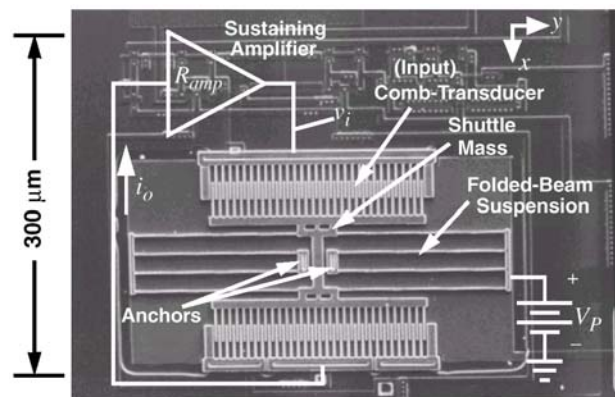


Fig. 3: SEM of a fully integrated 16-kHz watch oscillator that combines CMOS and MEMS in a single fully planar process [15].

With this in mind, Fig. 2 presents key cross-sections describing a polysilicon surface micromachining process done directly over silicon CMOS circuits in a modular fashion, where process steps for the transistor and MEMS portions are kept separate, in distinct modules [15]. (Modularity is highly desirable in such a process, since a modular process can more readily adapt to changes in a given module, e.g., to a new CMOS channel length.) As shown, this process entails depositing and patterning films above a finished CMOS circuit using the same equipments already found in CMOS foundries until a cross section as in Fig. 2(a) is achieved. Here, the structural polysilicon layer has been temporarily supported by a sacrificial oxide film during its own deposition and patterning. After achieving the cross-section of Fig. 2(a), the whole wafer is dipped into an isotropic etchant, in this case hydrofluoric acid, which attacks only the oxide sacrificial layer, removing it and leaving the structural polysilicon layer intact, free to move.

Fig. 3 presents the SEM of a watch oscillator that combines a 16 kHz folded-beam micromechanical resonator with a Q of 50,000 together with sustaining CMOS transistor circuits using the very process flow of Fig. 2, but with tungsten as the metal interconnect in order to accommodate 625°C structural polysilicon deposition temperatures [15].

Although the use of tungsten instead of the more conventional copper and aluminum prevents the process of [15] from widespread use, other variants of this modular process have now been demonstrated that allow more conventional CMOS metals [16]. In addition, other non-modular merging processes [17] have already been used in integrated MEMS products for many years now. Whichever process is used, the size and integration benefits are clear, as the complete timekeeper of Fig. 3 measures only $300 \times 300 \mu\text{m}^2$, and could even be smaller if the transistors were placed underneath the micromechanical structure.

III. VIBRATING MICROMECHANICAL RESONATORS

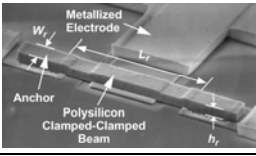
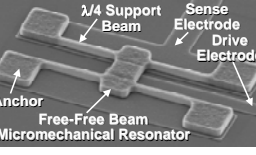
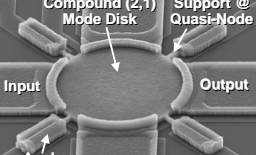

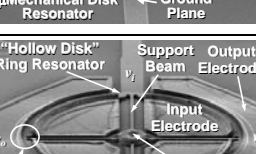
Because mechanical resonances generally exhibit orders of magnitude higher Q than their electrical counterparts, off-chip vibrating mechanical resonators (e.g., quartz crystals, SAW resonators) capable of achieving Q 's $>1,000$ are already essential components in communication circuits. With appropriate scaling via MEMS technology, such devices can not only be integrated alongside transistors on a single-chip, but can also be designed to vibrate over a very wide frequency range, from 1 kHz to >1 GHz, making them ideal for ultra stable oscillator and low loss filter functions at common transceiver frequencies. On this point, as will be detailed in Section IV, resonator types that allow specification of frequency via CAD-definable parameters (e.g., *lateral*, rather than thickness, dimensions) are most attractive, since they allow realization of many different frequencies in a single layer.

A. Capacitively Transduced Micromechanical Resonators

Among lateral-mode micromechanical resonators, capacitively transduced ones so far exhibit the highest frequency- Q products, since they generally are constructed in single high quality materials, and thus suffer less from the material interface losses that can encumber other transducer types (e.g., piezoelectric). In addition to better Q , capacitive transduction also offers more flexible geometries with CAD-definable frequencies, voltage-controlled reconfigurability [18][19], better thermal stability [9], material compatibility with integrated transistor circuits, and an on/off self-switching capability [19], all of which contribute to a strong amenability to mechanical circuit design.

Table 1 succinctly presents the evolution of capacitively transduced vibrating micromechanical resonator geometries over the past ten years. As shown, clamped-clamped beam resonators (row 1 of Table 1), which are essentially guitar strings scaled down to μm dimensions to achieve VHF frequencies, can achieve on-chip Q 's $\sim 8,000$ for oscillator and filtering functions in the HF range. However, anchor losses in this specific structure begin to limit the achievable Q at

TABLE 1: HIGH FREQUENCY- Q PRODUCT VIBRATING RF MEMS DEVICES

	Photo	Performance
CC-Beam Resonator [20]		Demo'ed: $Q \sim 8,000$ @ 10 MHz (vac) $Q \sim 50$ @ 10 MHz (air) $Q \sim 300$ @ 70 MHz (anchor diss.) Q drop w/ freq. limits freq. range Series Resistance, $R_x \sim 5-5,000\Omega$
FF-Beam Resonator [21]		Demo: $Q \sim 28,000$ @ 10-200 MHz (vac) $Q \sim 2,000$ @ 90 MHz (air) No drop in Q with freq. Freq. Range: >1 GHz; unlimited w/ scaling and use of higher modes Series Resistance, $R_x \sim 5-5,000\Omega$
Wine-Glass Disk Res. [22]		Demo'ed: $Q \sim 161,000$ @ 62 MHz (vac) $Q \sim 8,000$ @ 98 MHz (air) Perimeter support design nulls anchor loss to allow extremely high Q Freq. Range: >1 GHz w/ scaling Series Resistance, $R_x \sim 5-5,000\Omega$
Contour-Mode Disk Res. [6][7]		Demo'ed: $Q \sim 11,555$ @ 1.5 GHz (vac) $Q \sim 10,100$ @ 1.5 GHz (air) Balanced design and material mismatching anchor-disk design nulls anchor loss Freq. Range: >1 GHz; unlimited w/ scaling and use of higher modes Series Resistance, $R_x \sim 50-50,000\Omega$
Hollow Disk Ring Res. [8]		Demo'ed: $Q \sim 15,248$ @ 1.46 GHz (vac) $Q \sim 10,165$ @ 1.464 GHz (air) $\lambda/4$ notched support nulls anchor loss Freq. Range: >1 GHz; unlimited w/ scaling and use of higher modes Series Resistance, $R_x \sim 50-5,000\Omega$

higher VHF frequencies, limiting the practical range of this structure to <100 MHz when using μm -scale dimensions. To achieve higher frequency while retaining Q 's in the thousands and without the need for sub- μm dimensions [23] (which can potentially degrade the power handling and frequency stability of these devices in present-day applications [24]), more balanced structures that eliminate anchor losses can be used, such as the free-free beam [21] in row 2; the wine-glass [22] and contour-mode disks [6][7] in rows 3 and 4; and the ring [8] in row 5 of Table 1. The disks and ring of this group already operate beyond GHz frequencies with Q 's greater than 10,000 (in both vacuum and air), all while retaining sufficiently large dimensions to maintain adequate power handling and to avoid "scaling-induced" phenomena, such as mass-loading or temperature fluctuation noise [24], that might degrade performance when dimensions become too small.

The device of row 4 of Table 1 consists of a $20\mu\text{m}$ -diameter, $2\mu\text{m}$ -thick polydiamond disk suspended by a polysilicon stem self-aligned to be exactly at its center, all enclosed by polysilicon electrodes spaced 80 nm from the disk perimeter [6]. When vibrating in its radial contour mode, the disk expands and contracts around its perimeter in what effectively amounts to a high stiffness, high energy,

extensional mode. Since the center of the disk corresponds to a node location for the radial contour vibration mode shape, anchor losses through the supporting stem are greatly suppressed, allowing this design to retain a very high Q even at this UHF frequency. In addition to the GHz data shown in row 4 of Table 1, a version of this device at 498 MHz achieves a Q of 55,300 in vacuum [6], which corresponds to a frequency- Q product of 2.75×10^{13} —the highest for any resonator in the GHz range at room temperature. Furthermore, the high stiffness of its radial contour mode gives this resonator a much larger total (kinetic) energy during vibration than exhibited by previous resonators, making it less susceptible to energy losses arising from viscous gas damping, hence, allowing it to retain Q 's $>10,000$ even at atmospheric pressure. This resonator not only achieves a frequency applicable to the RF front ends of many commercial wireless devices, it also removes the requirement for vacuum to achieve high Q , which should greatly lower cost.

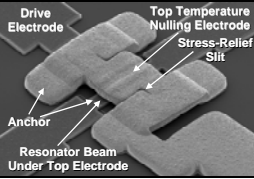
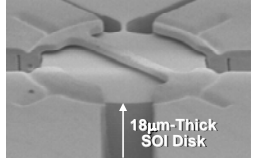
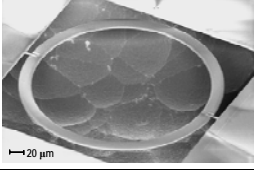
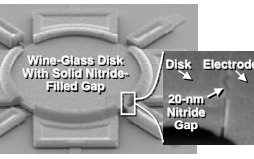
It should be noted that the disk of row 4 in Table 1 is constructed of polydiamond, which has twice the acoustic velocity of polysilicon, so facilitates the realization of GHz frequencies. However, polysilicon structures can also achieve similar performance when designed with the right geometry and isolating anchoring, as exemplified by the ring resonator of row 5 in Table 1, which uses a centrally located quarter-wavelength support structure with ring notches to minimize anchor losses towards Q 's $>10,000$ in both vacuum and air at 1.46 GHz [8].

B. Thermal Stability, Aging, and Impedance

Besides frequency range and Q , thermal stability, aging/drift stability, and impedance, are also of utmost importance. Table 2 presents some of the μ mechanical resonator devices designed specifically to address these parameters. In particular, the beam device of row 1 in Table 2 utilizes a temperature-tailored top electrode-to-resonator gap spacing to attain a total frequency deviation over 27-127°C of only 18 ppm, which actually betters that of AT quartz. This, combined with recent demonstrations of good aging and drift [10][11], makes μ mechanical resonators excellent candidates for reference oscillator applications in communication circuits. In addition, the devices of rows 2 and 3 illustrate strategies for lowering the impedances of stand-alone resonators, the first based on enlargement of the electrode-to-resonator capacitive overlap area to increase electromechanical coupling [25]; the second dispensing with capacitive transducers, and using piezoelectric transducers [12][26]; with the latter so far being the more successful in achieving the 50-377 Ω impedances desired for matching to off-chip components.

Although it does achieve low impedance, and is amenable to CAD specification, the piezoelectric device of row 3 in Table 2 still sacrifices the important high Q , on/off self-switching, and temperature stability attributes offered by

TABLE 2. THERMAL STABILITY AND IMPEDANCE OF MICRORESONATORS

	Photo	Performance
Electrical Stiff. Comp. Res. [9]		Demo'ed: $Q \sim 4,000$ @ 10MHz (vac) Temperature-tailored gap to effect an electrical stiffness variation that cancels Young's modulus variation 18 ppm freq. variation over 27-127°C
SOI Silicon WG-Disk [25]		WGDisk: $Q \sim 26,000$ @ 149MHz (air) SiBAR: $Q \sim 40,000$ @ 137 MHz (vac) $Q \sim 3,700$ @ 983 MHz SOI thickness to effect large capacitive overlap for low Series Resistance, $R_x \sim 5.5k\Omega$ @ 137 MHz
Lateral Piezoelec. Ring [12]		Demo'ed: $Q \sim 2,900$ @ 473 MHz (air) Contour-mode ring-shaped AlN piezoelectric resonator Driven laterally via the d_{31} coeff., so freqs. determined by lateral dims. Series Resistance, $R_x \sim 80\Omega$
Solid-Gap Disk Resonator [27]		Demo'ed: $Q \sim 25,300$ @ 61MHz (vac) Solid nitride-filled electrode-to-resonator gap (20 nm) Much better yield and able to achieve low impedance at low dc-bias voltage Series Resistance, $R_x \sim 1.5k\Omega$ @ 4V

capacitive transducers. To attain impedances similar to that of the row 3 device, yet retain capacitive transduction and all of its benefits, the device of row 4 has very recently been introduced. This 61-MHz wine-glass mode device is identical in shape and operation to that of row 3 in Table 1, but is now equipped with a solid dielectric-filled capacitive transducer gap (to replace the previous air gap) that reduces its impedance by 8 \times over its air-gap counterpart, while allowing it to retain a very high Q of 25,300 [27]. In addition to lower motional resistance, the use of solid dielectric-filled transducer gaps provides numerous other practical advantages over the air gap variety, since it (1) better stabilizes the resonator structure against shock and microphonics; (2) eliminates the possibility of particles getting into an electrode-to-resonator air gap, thereby removing a potential reliability issue; (3) greatly improves fabrication yield, by eliminating the difficult sacrificial release step needed for air gap devices; and (4) facilitates larger micromechanical circuits (e.g., bandpass filters comprised of interlinked resonators) by stabilizing constituent resonators as the circuits they comprise grow in complexity. Solid-dielectric capacitively transduced resonators employing a vertical-to-lateral drive, and thereby not requiring a nano-scale lateral gap, have also been successfully demonstrated [28].

IV. INTEGRATED MICROMECHANICAL CIRCUITS

Like single transistors, stand-alone vibrating micromechanical elements have limited functionality. To expand their functional range, micromechanical elements (like transistors) need to be combined into more complex circuits that

achieve functions better tailored to a specific purpose (e.g., frequency filtering, generation, or translation). Given that the property that allows transistors to be combined into large circuits is essentially their large gain, it follows that mechanical elements can be combined into equally large circuits by harnessing their large Q . As a simple example, transistor elements can be cascaded in long chains, because their gains compensate for the noise and other losses that would otherwise degrade the signal as it moves down the chain. On the other hand, mechanical elements can be cascaded into long chains because of their extremely low loss—a benefit of their high Q . In essence, if an element has an abundance of some parameter (i.e., gain, Q , ...), then this can generally be used to build circuits of that element.

The ingredients required for a micromechanical circuit technology comprise much more than just small size. For example, the piezoelectric thin-film bulk acoustic resonators (FBAR's) [13][14] that have already become a successful high volume product in the wireless handset arena, although small, are perhaps not suitable for large-scale circuit design, since their frequencies are governed almost entirely by thickness, which is not a parameter that can be specified via computer-aided design (CAD) layout. Given how instrumental CAD has been to the success of VLSI transistor IC design, one would expect CAD-amenability to be equally important for micromechanical IC's. In this respect, the resonators and other elements in the repertoire of a micromechanical circuit design environment should have frequencies or other characteristics definable by *lateral* dimensions easily specifiable by CAD.

Continuing on this theme, a more complete set of attributes needed to effect a micromechanical circuit design environment can be listed as follows:

- 1) *CAD-amenable design*. For example, frequencies should be determined by lateral dimensions, which can be specified via CAD, not just vertical dimensions, which cannot. This makes possible an ability to attain many different frequencies in a single layer on a single-chip.
- 2) *Geometric flexibility*. Here, a given (often high) frequency should be attainable in a wide variety of shapes (e.g., beams, disks, etc.) and modes.
- 3) *Q 's $>1,000$ from 1–5000 MHz, with Q 's $>10,000$ much preferred, if possible*. Q 's this high are needed to allow cascading of circuit blocks without accumulating excessive loss, and to allow channel-selection at RF.
- 4) *Thermal and aging stability to better than 2 ppm*, or at least amenable to compensation or control to this level.
- 5) *On/off switchability*. Here, the overriding preference is for vibrating micromechanical devices that can switch themselves, i.e., that do not require extra series switches, and that thus avoid the extra cost and insertion loss.
- 6) *Massive-scale interconnectivity*. In some cases, several levels of both mechanical and electrical interconnect are desired.
- 7) *Nonlinear characteristics* that enable such functions as

mixing, amplification, limiting, and other useful signal processing abilities.

- 8) *Amenability to low-capacitance single-chip integration with transistors*. This not only eliminates the impedance issue described previously, since the tiny magnitudes of on-chip parasitic capacitors allow impedances in the k Ω range, but also affords designers a much wider palette of mechanical and electrical circuit elements.

Devices with the above attributes and a path to the integration density illustrated in Fig. 3 have the potential to shift paradigms that presently constrain the number of high- Q components permissible in the design of portable wireless devices, and instead allow the use of hundreds, perhaps thousands (or more), of high- Q elements with negligible size or cost penalty. In particular, the devices of Table 1 and Table 2 sport many of the attributes and ingredients to realize a micromechanical circuit technology that could reach large-scale integrated (LSI), or even very large-scale integrated (VLSI), proportions, the same way integrated circuit (IC) transistors had done over recent decades, and with potential for advances in capabilities in the mechanical domain as enormous as those achieved via the IC revolution in the electrical domain.

V. MICROMECHANICAL CIRCUIT EXAMPLES

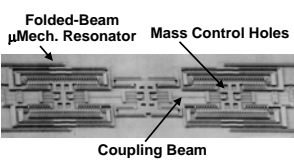
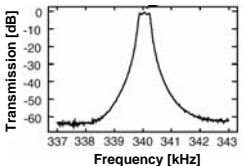
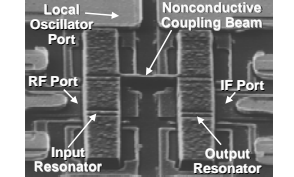
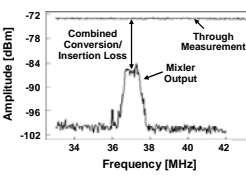
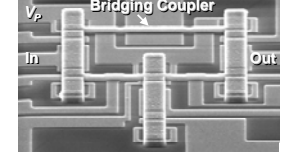
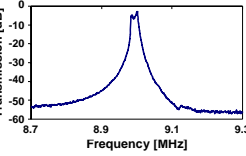
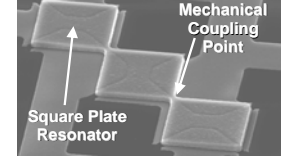
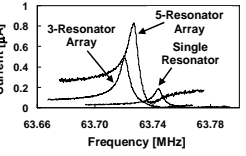
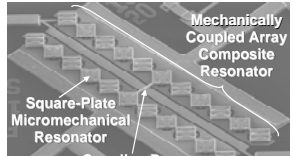
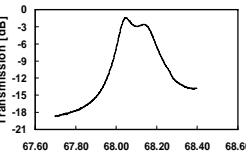
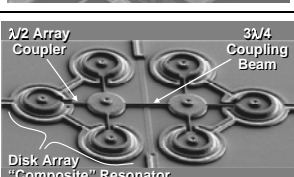
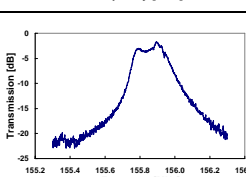
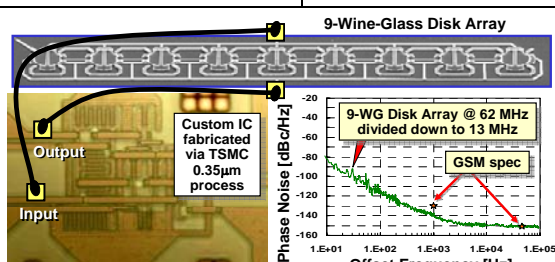
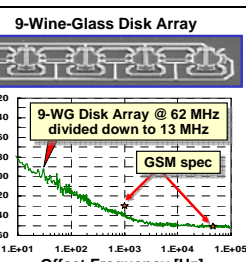
Given that they satisfy all of the attributes listed in Section IV, it is no surprise that capacitively transduced resonators have been used to realize many of the the most complex micromechanical circuits to date. Table 3 summarizes several purely micromechanical circuits, from bandpass filters with impressive on-chip insertion losses of only 0.6dB for 0.09% bandwidth [29], some using non-adjacent bridging to effect loss poles [30]; to mixer-filter ("mixler") devices that both translate and filter frequencies via a single passive structure [18]; to impedance transforming mechanically-coupled arrays that combine the responses of multiple high-impedance resonators to allow matching to a much lower 50 Ω [31]; to a filter using mechanically-coupled composite resonators to allow matching to 50 Ω while attaining the lowest insertion loss to date for a VHF micromechanical filter [32][33]; to an oscillator using a micromechanical disk array-composite resonator together with a custom-designed sustaining amplifier IC to achieve phase noise skirts compliant with GSM reference oscillator specifications [35].

Each of the filters in Table 3 is comprised of several identical resonator elements coupled by mechanical links attached at very specific locations on the resonators. As detailed more fully in [20] and [29], the center frequency of such a mechanical filter is determined primarily by the (identical) frequencies of its constituent resonators, while the spacings between modes (i.e., the bandwidth) is determined largely by a ratio of the stiffnesses of its coupling beams to that of the resonators they couple at their attachment locations. The circuit nature of each filter in Table 3 is emphasized by the fact that each was designed using equiva-

lent electrical circuits defined by electro-mechanical analogies [20][29], which allowed the use of electrical circuit simulators, like SPICE—an important point that implies mechanical circuits should be amenable to the vast automated circuit design environments already in existence. Fig. 4 presents the specific electric circuit equivalence for the bridged filter of row 3 of Table 3, where each flexural-mode resonator equates to an *LCR* circuit; each coupling beam is actually an acoustic transmission line, so equates to a *T*-network of energy storage elements, just like an electrical transmission line; the attachment locations of couplers to resonators must be chosen carefully, since they actually realize velocity transformations, which can again be modeled by transformers; the capacitive electromechanical transducers at the input and output ports equate to electrical transformers; and all circuit elements are specified by the lateral dimensions of their associated mechanical elements, making the whole structure amenable to automatic generation by a computer-aided design (CAD) program. Such a program could also automatically generate the layout required to achieve a specific filter specification, making the realization of a VLSI circuit of such filters as simple as already done for VLSI transistor IC's.

Although the filter of row 3 exhibits excellent in-band insertion loss and stop-band rejection, it requires a matching input termination impedance larger than 50Ω , making it unsuitable for placement directly after an antenna. As mentioned in Section III, this is a consequence of the use of weak air-gap capacitive transducers, which can be remedied using some of the methods presented in Table 2 [28][33] [34]. But there is another, perhaps more elegant, circuit-based remedy based on arraying. In particular, the arraying used in the devices of rows 4 and 5 not only provides a lower filter termination impedance by increasing the effective capacitive transducer overlap area, but also raises the 3rd order intermodulation intercept point (IP_3) of the composite device [36][37][38] (i.e., raises its linearity) in the process. Fig. 5 further illustrates how arraying can achieve a much larger increase in capacitive transducer overlap area than a single device specially designed for larger transducer area—a clear example of how a circuit technique can be superior to the use of a single

TABLE 3: SUMMARY OF VIBRATING MICROMECHANICAL CIRCUITS

	Photo	Data	Performance
3-Res. Folded-Beam Filter [29]			Freq. = 340 kHz BW = 403 Hz %BW = 0.09% StopB Rej. = 64 dB Ins. Loss < 0.6 dB
Mixer-Filter [18]			Mixes a 240MHz RF down to 37MHz IF, then filters Conv. Loss = 9.5dB %BW = 1.7% Ins. Loss = 3.5dB
3 Res. Bridged CC-Beam [30]			Freq. = 9 MHz BW = 20 kHz %BW = 0.2% StopB Rej. = 51 dB Ins. Loss < 2.8 dB
Mech.-Coupled Res. Array [31]			Automatic matching of resonators achieved via mech. coupling; current multiplied by number of resonators <i>N</i>
Array Composite Filter [32]			Freq. = 68.1 MHz BW = 190 kHz %BW = 0.28% StopB Rej. = 25 dB Ins. Loss < 2.7 dB
Disk Array Comp. Filter [33]			Freq. = 156 MHz BW = 201 kHz %BW = 0.13% StopB Rej. = 22 dB Ins. Loss < 2 dB
Disk Array Composite Oscillator [35]			Freq. = 62 MHz 9-Wine-Glass-Disk Composite Array Resonator Custom IC $L\{f_m=1\text{kHz}\} = -140\text{dBc}$ $L\{f_m=10\text{kHz}\} = -150\text{dBc}$

“advanced” device. The similarities between the described arraying approach and similar strategies in transistor integrated circuit design are noteworthy. In particular, the use of an array of resonators to match the impedance of a micro-mechanical circuit to an off-chip macroscopic element (e.g., an antenna) is really no different from the use of a cascade of progressively larger inverters (or in actual layout, arrays of smaller inverters) to allow a minimum-sized digital gate

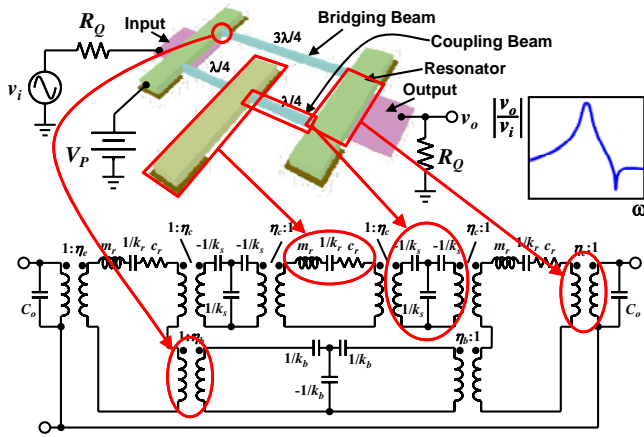


Fig. 4: Equivalent circuit and explicit mechanical-to-electrical equivalence for the bridged micromechanical filter of row 3 in Table 3.

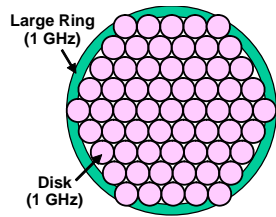


Fig. 5: Illustration showing that, in the same footprint, an array of small 1GHz disks can achieve a larger sidewall surface area (hence, larger electromechanical coupling and smaller filter impedance) than a single 1GHz ring made large to minimize impedance.

to drive an off-chip board capacitor. In essence, micro (or nano) scale circuits, whether they be electrical or mechanical, prefer to operate with higher impedances than macro-scale ones, and interfacing one with the other requires a proper impedance transformation. In a building block circuit environment, such an impedance transformation is most conveniently accomplished via large numbers of circuit elements, whether they be electronic transistors or mechanical resonators.

Again, it is the amenability to CAD of vibrating RF MEMS technology that makes the purely mechanical filters and arrays of Table 3 possible, and it is this same amenability to CAD that stands to effect substantial reductions in both cost and size for multi-band, multi-mode transceivers like that of Fig. 1. In particular, the tiny size and high integration density of micromechanical circuit technology makes the chip of Fig. 6 possible, which includes all the high- Q filters and resonators of Fig. 1 in a chip size of only $0.25\text{mm} \times 0.5\text{mm}$. Furthermore, if the on-chip passives technology used in Fig. 6 is indeed one where device properties (e.g., frequencies) can be specified by CAD-definable quantities (e.g., lateral dimensions, as opposed to thickness), allowing them to be defined in a single deposited layer, then the cost of a single chip of all 11 of the high- Q passives in Fig. 1 could potentially end up being about the same as one of the original off-chip passives. Needless to say, this degree of cost reduction creates great incentive for development of lateral vibration-mode MEMS resonators, for which frequency is defined by CAD-definable lateral dimensions; as opposed to thickness mode resonators (e.g., FBAR's or shear-mode quartz) that require a different film

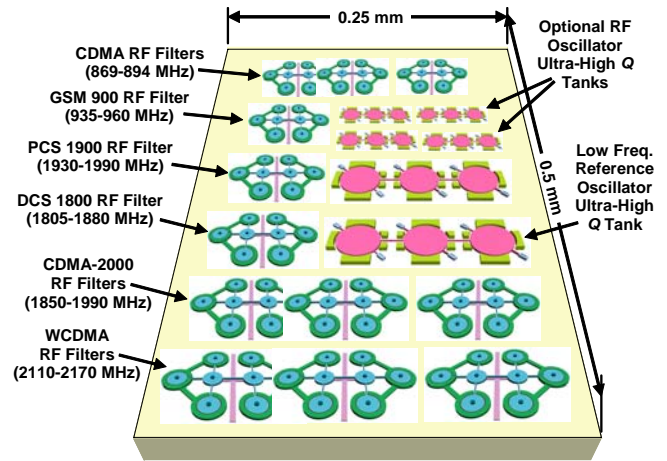


Fig. 6: Schematic of a single-chip of high- Q passives made possible by lateral-mode vibrating MEMS resonator technology. Here, a resonator technology that allows many different frequencies to be defined (e.g., via CAD layout) in a single film layer is assumed. The above $0.25 \times 0.5 \text{mm}^2$ chip includes the receive path high- Q passives of Fig. 1, plus additional oscillator tanks for improved phase noise and injection locking suppression. Although only receive path high- Q filters are included, here, note that transmit filters, as well as other lateral-dimension-defined passives described in this paper, could also be added while still retaining a tiny chip size.

thickness for each individual frequency, and thus, impose higher cost. If the lateral-mode resonators further use capacitive transduction, then they possess the additional advantage of self-switchability [19], which allows the system of Fig. 1 to dispense with the multi-throw switch, and hence, dispense with its size, cost, and insertion loss.

A. Combined MEMS-Transistor Circuits

Even greater capability becomes possible if transistors can be added to these mechanical circuits. The oscillator in row 7 of Table 3 [35] is one good example where the use of a micromechanical circuit improves the performance of a combined MEMS-transistor circuit. In this particular oscillator, the use of a disk array-composite resonator raises the power handling of the effective resonant tank element while retaining a very high Q of 118,900. Since Leeson's equation [39] indicates that the stability of an oscillator, as measured by its phase noise, is inversely proportional to the Q of its frequency setting tank element and to the power circulating through the oscillator feedback loop, the use of a disk array-composite to increase the power- Q product over that of a stand-alone resonator constitutes a mechanical circuit technique that can very effectively improve the phase noise performance of any oscillator. This mechanical circuit technique is in fact responsible for lowering the phase noise of the oscillator in row 7 of Table 3 to -140 dBc/Hz at 1 kHz offset from a 13-MHz carrier, and -150 dBc/Hz at far-from-carrier offsets, both of which together satisfy the GSM reference oscillator requirement [35].

The implications of this go far beyond merely satisfying present-day specifications. Given that the micromechanical disk and ring resonators of rows 4 and 5 of Table 1 have posted the highest room temperature Q 's of any on-chip

resonator around 1 GHz to date, the use of MEMS technology in compact local oscillator (LO) implementations is fully expected to yield substantial improvements in LO performance. In particular, according to Leeson's equation, if a present-day VCO attains -121 dBc/Hz at a 600 kHz offset from an 1.8 GHz carrier using an LC tank with a Q of 30, then the use of a vibrating micromechanical disk resonator with a Q of 10,000 should provide an astonishing ~ 50 dB of improvement, or -171 dBc/Hz at a 600 kHz carrier offset (provided the thermal noise floor allows it).

B. Micro-Oven Control

In addition to good short-term stability, MEMS technology has great potential to achieve oscillators with excellent thermal stability. In particular, the tiny size and weight of vibrating micromechanical resonators allow them to be mounted on micro-platforms suspended by long thin tethers with thermal resistances many orders of magnitude larger than achievable on the macro-scale. Such a large thermal resistance to its surroundings then allows the platform and its mounted contents to be heated to elevated temperatures with very little power consumption (e.g., milliwatts). Fig. 1 presents the first such platform-mounted folded-beam micromechanical resonator, where the nitride platform supporting the resonator also included thermistor and heating resistors that when embedded in a feedback loop that kept the temperature of the platform at 130°C with only 2mW of total power consumption [40]. With oven-controlling feedback engaged, the temperature coefficient of the platform-mounted micromechanical resonator was reduced by more than 5 times, with thermally induced warping of the platform the performance limiter. Much better reduction factors are expected with a more refined platform design.

VI. LARGE-SCALE INTEGRATED (LSI) MICROMECHANICAL CIRCUITS

Again, to fully harness the advantages of μ mechanical circuits, one must first recognize that due to their micro-scale size and zero dc power consumption, μ mechanical circuits offer the same system complexity advantages over off-chip discrete passives that planar IC circuits offer over discrete transistor circuits. Thus, to maximize performance gains, μ mechanical circuits should be utilized on a massive scale. Again, as with transistor circuits, LSI (and perhaps eventually VLSI) mechanical circuits are best achieved by hierarchical design based on building block repetition, where resonator, filter, or mixer-filter building blocks might be combined in a similar fashion to the memory cell or gate building blocks often used in VLSI transistor IC's.

One example of an LSI micromechanical circuit expected to impact future transceivers is the RF channel selector mentioned in Section I and described at the system-level in [3] and [4]. Such an RF channel-selector, if achievable, is widely coveted by RF designers. Indeed, if channel-selection (rather than band-selection) were possible at RF

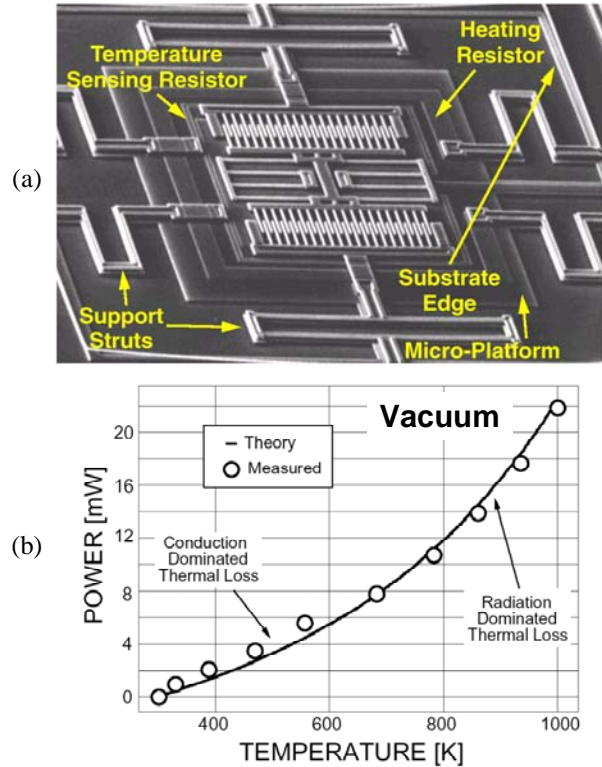


Fig. 1: (a) SEM of a fabricated folded-beam micromechanical resonator mounted on a micro-oven platform. (b) Measured power required to achieve a given temperature. Here, only 2 mW is required to achieve 130°C [40].

frequencies (rather than just at IF), then succeeding electronic blocks in the receive path (e.g., LNA, mixer) would no longer need to handle the power of alternate channel interferers. This would greatly enhance the robustness of the receiver by raising its immunity against jamming. In addition, without alternate channel interferers, the dynamic range of the RF LNA and mixer can be greatly relaxed, allowing substantial power reductions. The absence of interferers also allows reductions in the phase noise requirements of the local oscillator (LO) synthesizer required for down-conversion, providing further power savings.

To date, RF channel selection has been difficult to realize via present-day technologies. In particular, low-loss channel selection at RF would require tunable resonators with Q 's $>10,000$. Unfortunately, such Q 's have not been available in the sizes needed for portable applications. In addition, high- Q often precludes tunability, making RF channel selection via a single RF filter a very difficult prospect. On the other hand, it is still possible to select individual RF channels via many non-tunable high- Q filters, one for each channel, and each switchable by command. Depending upon the communication standard, this could entail hundreds or thousands of filters—numbers that would be absurd if off-chip macroscopic filters are used, but that may be perfectly reasonable for micro-scale, passive, μ mechanical filters. In the scheme of Fig. 7, a given filter (or set of them) is switched on (with all others off) by de-

coder-controlled application of an appropriate dc-bias voltage to the desired filter. (From [19], a capacitively transduced resonator is on only when a finite dc-bias V_P is applied; i.e., with $V_P = 0V$, the device is effectively an open circuit.)

The potential benefits afforded by this RF channel selector can be quantified by assessing its impact on the LNA linearity specification imposed by a given standard, e.g., the IS-98-A interim standard for CDMA cellular mobile stations [41]. In this standard, the required IIP_3 of the LNA is set mainly to avoid desensitization in the presence of a single tone (generated by AMPS [42]) spaced 900 kHz away from the CDMA signal center frequency. Here, reciprocal mixing of the local oscillator phase noise with the 900 kHz offset single tone and cross-modulation of the single tone with leaked transmitter power outputs dictate that the LNA IIP_3 exceeds +7.6dBm [42]. However, if an RF channel select filter bank such as shown in Fig. 7 precedes the LNA and is able to reject the single tone by 40dB, the requirement on the LNA then relaxes to $IIP_3 \leq -29.3\text{dBm}$ (assuming the phase noise specification of the local oscillator is *not* also relaxed). Given the well-known noise versus power trade-offs available in LNA design [43], such a relaxation in IIP_3 can result in nearly an order of magnitude reduction in power. In addition, since RF channel selection relaxes the overall receiver linearity requirements, it may become possible to put more gain in the LNA to suppress noise figure (NF) contributions from later stages, while relaxing the required NF of the LNA itself, leading to further power savings.

VII. CONCLUSIONS

MEMS-based realizations of wireless transceiver functions, including 0.09% bandwidth filters with less than 0.6dB insertion loss, GSM-phase-noise-compliant oscillators, and mixer-filters that mix and IF filter in single passive devices, have been described with an emphasis on the performance benefits afforded by scaling to micro dimensions. In particular, via scaling, vibrating RF MEMS devices have now reached frequencies commensurate with critical RF functions in wireless applications and have done so with previously unavailable on-chip Q 's exceeding 10,000. Q 's this high may now encourage paradigm-shifting communication architectures that can eliminate interferers immediately after the antenna, allowing subsequent electronics to operate with much lower dynamic range and power consumption than would otherwise be needed. Given present transistor scaling trends towards lower dynamic range digital devices, such a relaxation in dynamic range requirements may be arriving at an opportune time.

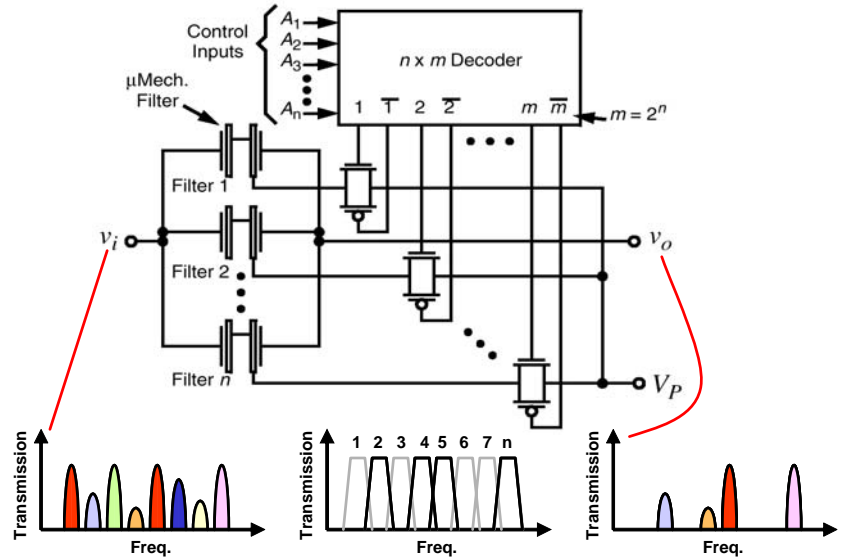


Fig. 7: Schematic diagram for an RF channel-select micromechanical filter bank, with an example showing how various input frequencies can be simultaneously selected via mere application or removal of resonator dc-biases. In the bottom plots, filters 2, 4, 5, and n are on, while all others are off.

At present, micromechanical circuit complexity is nearing medium-scale integration (MSI) density, as exemplified by the composite array filter in row 5 of Table 3, which uses more than 43 resonators and links. Indeed, circuit complexity and frequency range should only increase as MEMS technologies evolve into NEMS (or "nanoelectromechanical system") technologies, with feature sizes that support frequencies exceeding 10 GHz. In fact, with knowledge of the micromechanical circuit concepts described herein, one might now even question the numerous ongoing research efforts to make transistors out of nanowires. One might ask: Why do this? After all, nanowires can be employed more naturally as vibrating resonators capable of doing mechanical signal processing when mechanically linked into circuit networks similar to those described herein. Such nanomechanical networks would not only be completely passive, consuming substantially less power, but would also dispense with the need for the electrical contacts that presently inhibit large scale integration of nanowire transistors.

REFERENCES

- [1] A. A. Abidi, "Direct-conversion radio transceivers for digital comms," *IEEE J. Solid-State Circuits*, vol. 30, No. 12, pp. 1399-1410, Dec. 1995.
- [2] C.P. Yue and S.S. Wong, "On-chip spiral inductors with patterned ground shields for Si-based RF IC's," *IEEE J. Solid-State Circuits*, vol. 33, no. 5, pp.743-752, May 1998.
- [3] C. T.-C. Nguyen, "Transceiver front-end architectures using vibrating micromechanical signal processors," chapter in *RF Technologies for Low Power Wireless Communications*, edited by G. I. Haddad, T. Itoh, and J. Harvey, pp. 411-461. New York: Wiley IEEE-Press, 2001.
- [4] C. T.-C. Nguyen, "Vibrating RF MEMS overview: applications to wireless communications (invited)," *Proceedings, Photonics West: MOEMS-MEMS 2005*, San Jose, California, Jan. 22-27, 2005, Paper No. 5715-201.
- [5] C. T.-C. Nguyen, "Vibrating RF MEMS for next generation wireless applications," *Proceedings, 2004 IEEE Custom Integrated Circuits*

C. T.-C. Nguyen, "Integrated micromechanical circuits for RF front ends," *Proceedings of the 36th European Solid-State Device Research Conference*, Montreux, Switzerland, Sept. 19-21, 2006, pp. 7-16.

- Conf., Orlando, Florida, Oct. 3-6, 2004, pp. 257-264.
- [6] J. Wang, J. E. Butler, T. Feygelson, and C. T.-C. Nguyen, "1.51-GHz polydiamond micromechanical disk resonator with impedance-mismatched isolating support," *Proceedings, 17th Int. IEEE Micro Electro Mechanical Systems Conf.*, Maastricht, The Netherlands, Jan. 25-29, 2004, pp. 641-644.
- [7] J. Wang, Z. Ren, and C. T.-C. Nguyen, "1.156-GHz self-aligned vibrating micromechanical disk resonator," *IEEE Trans. Ultrason., Ferroelect., Freq. Contr.*, vol. 51, no. 12, pp. 1607-1628, Dec. 2004.
- [8] S.-S. Li, Y.-W. Lin, Y. Xie, Z. Ren, and C. T.-C. Nguyen, "Micromechanical hollow-disk ring resonators," *Proceedings, IEEE Int. MEMS Conf.*, Maastricht, The Netherlands, Jan. 25-29, 2004, pp. 821-824.
- [9] W.-T. Hsu and C. T.-C. Nguyen, "Stiffness-compensated temperature-insensitive μ mechanical resonators," *Tech. Dig.*, IEEE Int. MEMS Conf., Las Vegas, Nevada, Jan. 20-24, 2002, pp. 731-734.
- [10] V. Kaajakari, J. Kiihamäki, A. Oja, H. Seppä, S. Pietikäinen, V. Kokkala, and H. Kuisma, "Stability of wafer level vacuum encapsulated single-crystal silicon resonators," *Dig. of Tech. Papers*, Int. Conf. on Solid-State Sensors, Actuators, and Microsystems (Transducers'05), Seoul, Korea, June 2005, pp. 916-919.
- [11] B. Kim, R. N. Candler, M. Hopcroft, M. Agarwal, W.-T. Park, and T. W. Kenny, "Frequency stability of wafer-scale encapsulated MEMS resonators," *Dig. of Tech. Papers*, Int. Conf. on Solid-State Sensors, Actuators, and Microsystems (Transducers'05), Seoul, Korea, June 2005, pp. 1965-1968.
- [12] G. Piazza, *et al.*, "Low motional resistance ring-shaped contour-mode aluminum nitride piezoelectric micromechanical resonators for UHF applications," *Tech. Dig.*, 18th IEEE Int. Conf. on MEMS, Miami Beach, Florida, Jan. 30-Feb. 3, 2005, pp.20-23.
- [13] R. C. Ruby, P. Bradley, Y. Oshmyansky, A. Chien, and J. D. Larson III, "Thin film bulk wave acoustic resonators (FBAR) for wireless applications," *Proceedings, IEEE Int. Ultrasonics Symposium*, Atlanta, GA, 2001, pp. 813-821.
- [14] H. Yu, *et al.*, "Film bulk acoustic resonator at 4.4 GHz with ultra low temperature coefficient of resonant frequency," *Tech. Dig.*, IEEE Int. MEMS Conf., Miami Beach, Florida, Jan. 30-Feb. 3, 2005, pp. 28-31.
- [15] C. T.-C. Nguyen and R. T. Howe, "An integrated CMOS micromechanical resonator high-Q oscillator," *IEEE J. Solid-State Circuits*, vol. 34, no. 4, pp. 440-455, April 1999.
- [16] A. E. Franke, J. M. Heck, T.-J. King and R. T. Howe, "Polycrystalline silicon-germanium films for integrated microsystems," *IEEE/ASME J. Microelectromech. Syst.*, vol. 12, no. 2, pp. 160-171, April 2003.
- [17] T. A. Core, W. K. Tsang, and S. J. Sherman, "Fabrication technology for an integrated surface-micromachined sensor," *Solid State Technology*, pp. 39-47, Oct. 1993.
- [18] A.-C. Wong and C. T.-C. Nguyen, "Micromechanical mixer-filters ("mixlers")," *IEEE/ASME J. Microelectromech. Syst.*, vol. 13, no. 1, pp. 100-112, Feb. 2004.
- [19] S.-S. Li, Y.-W. Lin, Z. Ren, and C. T.-C. Nguyen, "Self-switching vibrating micromechanical filter bank," *Proceedings, IEEE Combined Int. Frequency Control/Precision Time & Time Interval Symposium*, Vancouver, Canada, Aug. 29-31, 2005, pp. 135-141.
- [20] F. D. Bannon III, J. R. Clark, and C. T.-C. Nguyen, "High frequency micromechanical filters," *IEEE J. Solid-State Circuits*, vol. 35, no. 4, pp. 512-526, April 2000.
- [21] K. Wang, A.-C. Wong, and C. T.-C. Nguyen, "VHF free-free beam high-Q micromechanical resonators," *IEEE/ASME J. Microelectromech. Syst.*, vol. 9, no. 3, pp. 347-360, Sept. 2000.
- [22] M. A. Abdelmoneum, M. U. Demirci, and C. T.-C. Nguyen, "Stemless wine-glass-mode disk micromechanical resonators," *Proceedings, 16th Int. IEEE MEMS Conf.*, Kyoto, Japan, Jan. 19-23, 2003, pp. 698-701.
- [23] X. M. H. Huang, C. A. Zorman, M. Mehregany, M. L. Roukes, "Nanodevice motion at microwave freqs," *Nature*, vol. 421, pg. 496, Jan. 30, 2003.
- [24] J. R. Vig and Y. Kim, "Noise in microelectromechanical system resonators," *IEEE Trans. Ultrason. Ferroelec. Freq. Contr.*, vol. 46, no. 6, pp. 1558-1565, Nov. 1999.
- [25] S. Pourkamali, *et al.*, "Vertical capacitive SiBARs," *Tech. Dig.*, 18th IEEE Int. Conf. on MEMS, Miami Beach, Florida, Jan. 30-Feb. 3, 2005, pp. 211-214.
- [26] D. T. Chang, *et al.*, "A new MEMS-based quartz resonator technology," *Tech. Dig.*, Solid-State Sensor, Actuator, and Microsystems Workshop, Hilton Head, South Carolina, June 6-10, pp. 41-44.
- [27] Y.-W. Lin, S.-S. Li, Z. Ren, and C. T.-C. Nguyen, "Vibrating micromechanical resonators with solid dielectric capacitive-transducer 'gaps'," *Proceedings, Joint IEEE Int. Freq. Control/Precision Time & Time Interval Symposium*, Vancouver, Canada, Aug. 29-31, 2005, pp. 128-134.
- [28] D. Weinstein, H. Chandrahali, L. F. Cheow and S. A. Bhawe, "Dielectrically transduced single-ended to differential MEMS filter," *Tech. Digest, 2006 IEEE Int. Solid-State Circuits Conf.*, San Francisco, California, February 5-9, 2006, pp. 318-319.
- [29] K. Wang and C. T.-C. Nguyen, "High-order medium frequency micromechanical electronic filters," *IEEE/ASME J. Microelectromech. Syst.*, vol. 8, no. 4, pp. 534-557, Dec. 1999.
- [30] S.-S. Li, *et al.*, "Bridged micromechanical filters," *Proceedings, IEEE Int. Ultrasonics, Ferroelectrics, and Freq. Control 50th Anniv. Joint Conf.*, Montreal, Canada, Aug. 24-27, 2004, pp. 144-150.
- [31] M. U. Demirci, M. A. Abdelmoneum, and C. T.-C. Nguyen, "Mech. corner-coupled square microresonator array for reduced series motional resistance," *Dig. of Tech. Papers*, Transducers'03, Boston, MA, June 8-12, 2003, pp. 955-958.
- [32] M. U. Demirci and C. T.-C. Nguyen, "A low impedance VHF micromechanical filter using coupled-array composite resonators," *Dig. of Tech. Papers*, the 13th Int. Conf. on Solid-State Sensors & Actuators (Transducers'05), Seoul, Korea, June 5-9, 2005.
- [33] S.-S. Li, Y.-W. Lin, Z. Ren, and C. T.-C. Nguyen, "Disk-array design for suppression of unwanted modes in micromechanical composite-array filters," *Tech. Digest, 19th IEEE Int. Conf. on MEMS*, Istanbul, Turkey, Jan. 22-26, 2006, pp. 866-869.
- [34] P. J. Stephanou, G. Piazza, C. D. White, M. B. J. Wijesundara, and A. P. Pisano, "Mechanically coupled contour mode piezoelectric aluminum nitride MEMS filters," *Tech. Digest, 2006 IEEE Int. MEMS Conf.*, Istanbul, Turkey, Jan. 22-26, pp. 906-909.
- [35] Y.-W. Lin, S.-S. Li, Z. Ren, and C. T.-C. Nguyen, "Low phase noise array-composite micromechanical wine-glass disk oscillator," *Tech. Digest, IEEE Int. Electron Devices Mtg.*, Washington, DC, Dec. 5-7, 2005, pp. 287-290.
- [36] R. Navid, J. R. Clark, M. Demirci, and C. T.-C. Nguyen, "Third-order intermodulation distortion in capacitively-driven CC-beam micromechanical resonators," *Tech. Digest, 14th Int. IEEE MEMS Conf.*, Interlaken, Switzerland, Jan. 21-25, 2001, pp. 228-231.
- [37] Y.-W. Lin, S.-S. Li, Z. Ren, and C. T.-C. Nguyen, "Third-order intermodulation distortion in capacitively-driven VHF micromechanical resonators," *Proceedings, IEEE Int. Ultrasonics Symposium*, Sept. 18-21, 2005, pp. 1592-1595.
- [38] A. T. Alastalo and V. Kaajakari, "Intermodulation in capacitively coupled microelectromechanical filters," *IEEE Electron Device Lett.*, vol. 26, no. 5, pp. 289-291, May 2005.
- [39] D. B. Leeson, "A simple model of feedback oscillator noise spectrum," *Proc. IEEE*, vol. 54, pp. 329-330, Feb. 1966.
- [40] C. T.-C. Nguyen and R. T. Howe, "Microresonator frequency control and stabilization using an integrated micro oven," *Dig. of Tech. Papers*, the 7th International Conference on Solid-State Sensors and Actuators (Transducers'93), Yokohama, Japan, pp. 1040-1043, June 7-10, 1993.
- [41] "Recommended minimum performance standards for dual-mode wide-band spread spectrum cellular mobile stations," *TIA/EIA/IS-98-A Interim Standard*, July 1996.
- [42] W. Y. Ali-Ahmad, "RF system issues related to CDMA receiver specifications," *RF Design*, pp. 22-32, Sept. 1999.
- [43] D. K. Shaeffer and T. H. Lee, "A 1.5-V, 1.5-GHz CMOS low noise amplifier," *IEEE J. Solid-State Circuits*, vol. 32, No. 5, pp. 745-759, May 1997.